

## Co-location of lightning leader x-ray and electric field change sources

J. Howard,<sup>1</sup> M. A. Uman,<sup>1</sup> J. R. Dwyer,<sup>2</sup> D. Hill,<sup>1</sup> C. Biagi,<sup>1</sup> Z. Saleh,<sup>2</sup> J. Jerauld,<sup>1,3</sup> and H. K. Rassoul<sup>2</sup>

Received 27 March 2008; revised 2 June 2008; accepted 12 June 2008; published 11 July 2008.

[1] Using an eight-station time of arrival (TOA) network composed of NaI(Tl) scintillation detectors and wideband electric field derivative ( $dE/dt$ ) antennas covering approximately  $1 \text{ km}^2$  on the ground, we have located both the sources of X-ray emissions and electric field changes produced during the leader phase of both downward negative natural and rocket-triggered lightning strokes. We show that the sources of X rays and leader step electric field changes are co-located in space within 50 m and that the located X rays are emitted 0.1 to 1.3  $\mu\text{s}$  after the origin of the leader step electric field changes. **Citation:** Howard, J., M. A. Uman, J. R. Dwyer, D. Hill, C. Biagi, Z. Saleh, J. Jerauld, and H. K. Rassoul (2008), Co-location of lightning leader x-ray and electric field change sources, *Geophys. Res. Lett.*, 35, L13817, doi:10.1029/2008GL034134.

### 1. Introduction

[2] Although X-ray emission from lightning was long predicted [Wilson, 1925], only recently was the production of X rays in cloud-to-ground lightning confirmed. Moore *et al.* [2001] first reported the detection of energetic radiation emissions immediately preceding the return stroke of natural cloud-to-ground negative lightning, followed by a similar discovery by Dwyer *et al.* [2003] for rocket-triggered lightning. Dwyer *et al.* [2004] reported that these emissions were composed of multiple, brief bursts of X rays in the 30–250 keV range, with each burst typically lasting less than 1  $\mu\text{s}$ . Further, they showed that the sources of the X-ray bursts traveled from the cloud toward the ground, supporting the view that the leader front is the source of the X rays. Dwyer *et al.* [2005] compared X-ray and electric field records simultaneously obtained during the stepped leaders of natural negative cloud-to-ground lightning. The conclusion from this analysis was that the production of X-rays is associated with the electric field changes accompanying the stepping of the leader that initiates the first return stroke. Although an obvious temporal correspondence was observed, uncertainties in measurement time delays and oscilloscope trigger times prevented any accurate determination of the exact temporal relationship between the X-ray bursts and the stepping of the leader. Observations of the similarity in X-ray emissions from natural and triggered lightning imply a common mechanism

for different types of negative leaders [Dwyer *et al.*, 2005]. The aforementioned discoveries have had an impact on views of lightning electrical breakdown in air, in that lightning can no longer necessarily be considered a conventional low-energy (eV) discharge, but often involves an electron distribution function that includes a significant high-energy (keV to MeV) component. These recent advancements highlight many unknowns regarding leader propagation, the stepping process, and their association with X rays. Among the most pressing of these issues are the intensity of the X rays at the source, the electric field at the leader front, the directionality and attenuation of the X-ray emissions, and the spatial and temporal relationship between the sources of X rays and leader steps. This paper addresses the issue of independently locating the sources of X-ray emissions and the corresponding leader step electric field changes via time-of-arrival (TOA) measurements, which may allow advancement on many of these issues. Leaders in both natural and triggered lightning are considered.

[3] Obtaining three dimensional locations for sources of lightning radiation from TOA measurements has been a developing science since Proctor [1971] pioneered the process using hyperbolic formulations. A more recent technique cast the nonlinear equations into a linear system whose solution can be viewed as the intersection of hyperplanes [Koshak and Solakiewicz, 1996]. Probably the most common approach, however, is to use the hyperplane technique to obtain an initial guess for a nonlinear least squares Marquardt algorithm [Koshak *et al.*, 2004; Thomas *et al.*, 2004]. Although such lightning mapping systems are typically applied to VHF radiation, other spectral ranges, such as wideband (800 Hz to 4 MHz, 6 dB)  $dE/dt$  [Thomson *et al.*, 1994], have been used. This paper reports the first attempt to utilize TOA techniques for locating lightning produced X rays.

### 2. Experiment

[4] The experiment discussed in this paper was conducted in 2006 and 2007 at the International Center for Lightning Research and Testing (ICLRT), an UF-FIT operated facility which occupies approximately  $1 \text{ km}^2$  at the Camp Blanding Army National Guard Base in north-central Florida. The eight-station TOA network described herein is a subset of the overall 24 station Multiple Station Experiment/Thunderstorm Energetic Radiation Array (MSE/TERA) which is presently being used to characterize the electromagnetic environment during nearby lightning. Each of the TOA stations, shown in Figure 1, contains a wideband (DC to 20 MHz, 3dB) flat plate electric field derivative antenna and a NaI/photomultiplier tube (PMT) detector.

<sup>1</sup>Department of Electrical and Computer Engineering, University of Florida, Gainesville, Florida, USA.

<sup>2</sup>Department of Physics and Space Sciences, Florida Institute of Technology, Melbourne, Florida, USA.

<sup>3</sup>Now at Raytheon Missile Systems, Tucson, Arizona, USA.

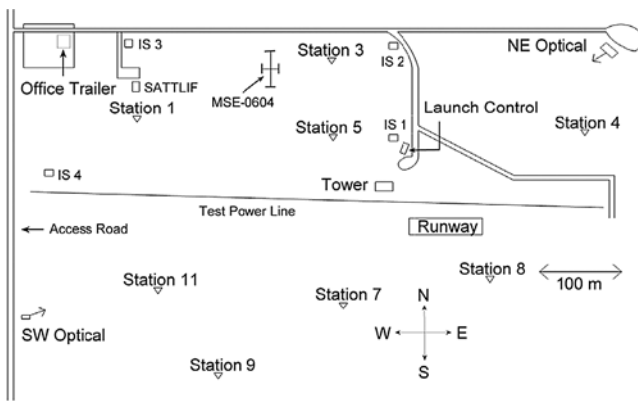


**Figure 1.** Layout of the eight-station (triangles) TOA network at the ICLRT along with the optical sensors used for triggering the network. The ground strike location for MSE-0604 is indicated with error bars near Station 3; UF-0707 was a rocket-triggered lightning which struck the Tower.

[5] The NaI detector is enclosed in an aluminum housing with a battery and associated electronics, similar to the system described by Dwyer *et al.* [2004]. The output of the flat plate antenna is fed into an underground metal enclosure also housing a battery and electronics. The X-ray detector housing and the flat plate antenna are separated by 10 m to avoid possible electric field enhancement. Both measurements are transmitted via fiber optics to Lecroy digital storage oscilloscopes, sampling at 250 MHz for 2 ms with 1 ms of pretrigger, located in a shielded trailer at the center of the site. The waveforms for the TOA network are stored on four oscilloscopes, with a fifth scope being used to synchronize their timebases. Optical sensors, placed at opposing corners of the network, are used to trigger the oscilloscopes at the time of on-site return strokes.

[6] The size of the TOA network must be relatively small due to the high attenuation (roughly 100 m e-folding distance) of X rays in the atmosphere; nevertheless, the stations were positioned to provide the largest practical geographic coverage. Highly accurate local coordinates were obtained for each measurement using an Electronic Total Station Traverse and a surveyor's level. Surveying errors for the flat plate antennas were less than the dimensions of the antennas themselves. Surveying errors were larger for the X-ray sensors ( $\sim 30$  cm) because locations were measured to the top center of the aluminum housing. Time delays for each measurement, from the sensor to the oscilloscope, were obtained to an accuracy of  $\sim 2$  ns using a system that directly measures the transit time for a test signal through each measurement.

[7] Waveforms of electric field derivatives and X rays are first synchronized to a single timebase and then each set is cross-correlated to aid in the identification of events across channels. Arrival times for  $dE/dt$  events are selected from the positive peak values, and times for X-ray events are manually selected from points of initial deflection in the waveforms. The set of times for each event must all occur within a small time window which is physically constrained by propagation paths and measurement time delays. Using these arrival times, all combinations for  $N \geq 5$  stations are

used in a nonlinear least squares Marquardt algorithm, similar to *Thomas et al.* [2004] and *Koshak et al.* [2004], to determine the location and time of occurrence for both types of sources. The final solution is selected based on the metric of the smallest product of the reduced chi-square value and location uncertainty of the solution. The location errors used in this metric are predicted from the covariance matrix returned from the solution algorithm. Due to the small network size, the hyperplane approach was not used to obtain an initial guess for the least squares algorithm; rather, a central point in the network at an altitude of 200 m above ground was used as the initial point for all solutions.

### 3. Results

[8] We report findings from one negative stepped leader, MSE-0604, occurring on 2 June 2006 and one negative rocket-triggered dart-stepped leader, UF-0707, occurring on 31 July 2007. The X-ray waveforms (prior to cross-correlation) involved in the solution for one event in MSE-0604 are shown in Figure 2, with the arrival times indicated by large arrows. These times correspond to deflections in the waveforms occurring within the allowable time window. As seen in both the Station 3 and Station 5 waveforms, it is possible for the response from multiple X-ray bursts to overlap due to the slow response of the NaI detectors. Therefore, there may be multiple possibilities for the arrival time on a particular channel, as indicated by the small arrows in Figure 2. Fortunately, cross-correlation of the waveforms typically places the correct times in the closest proximity to each other. Further, these times are generally separated in time enough that the incorrect values are seriously detrimental to the reduced chi-square value and the location errors, thus allowing them to be ruled out. Regardless, locating X-ray sources has proven far more challenging than locating leader steps from the electric field changes due to the low number of X-ray photons reaching the detectors given the relatively high X-ray attenuation in air and the relatively slow response of NaI detectors. This

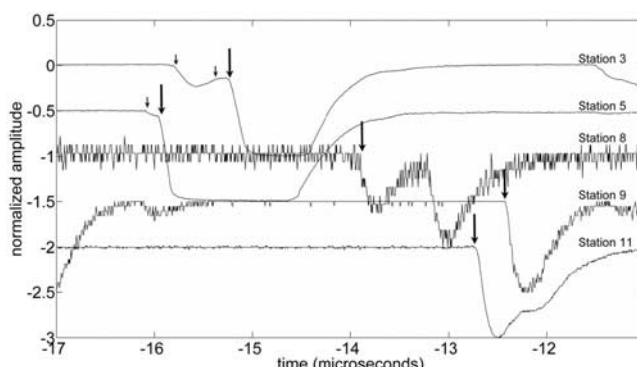


**Figure 2.** X-ray waveforms involved in the location of one event in MSE-0604. The arrival times used in the solution are indicated with large arrows. The bursts responsible for the arrival times on Station 3 and Station 5 produce responses which are superimposed on responses from uncorrelated bursts (small arrows). The waveforms are shown as recorded in Launch Control and prior to any correction for fiber optic time delays.

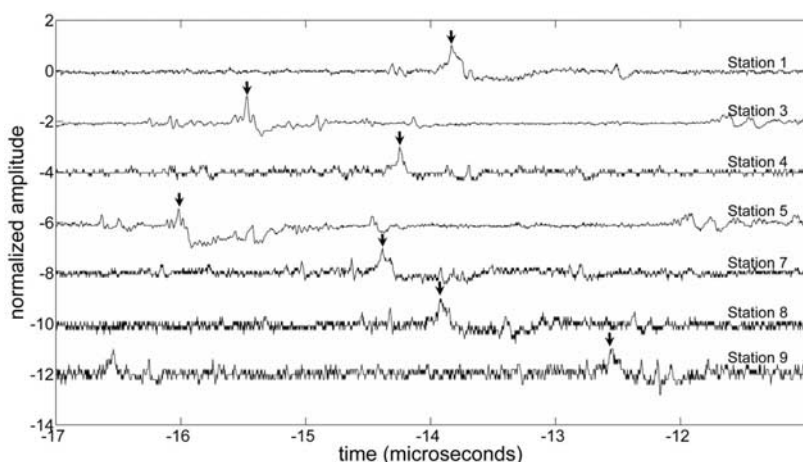


**Figure 3.** Electric field derivative waveforms corresponding to the X-ray pulses shown in Figure 2. The arrival times used for this event are indicated by the arrows.

fact is evident in the generally higher chi-square values, larger location uncertainties, and far fewer locatable sources for X rays than for electric field changes. Therefore, our method was to first identify locatable X-ray events (correlated detection on  $N \geq 5$  stations), determine the best solution based on our metric, and then determine the associated leader step location from  $dE/dt$  records. The  $dE/dt$  waveforms shown in Figure 3 are from the leader step associated with the X-ray emission shown in Figure 2. The arrival times, indicated with arrows, are selected from waveform peaks occurring within a restrictive time window, as noted above.

[9] The approximate location for MSE-0604, determined from averaging  $dE/dt$  source locations from the final 10 leader steps, is indicated in Figure 1 by the intersection of error bars in the  $x$  and  $y$  directions ( $\sigma_x = 10$  m and  $\sigma_y = 25$  m). This location is consistent with observed amplitudes

in electric field and electric field derivative measurements of the MSE. The  $dE/dt$  source locations for UF-0707 are in the volume above the Tower, shown in Figure 1, from which the rocket initiating the lightning was launched. For these two flashes, seven total X-ray/ $dE/dt$  source pairs were identified, three from flash MSE-0604 and four from UF-0707. The local source coordinates ( $x$ ,  $y$ ,  $z$ ), time of occurrence relative to trigger time ( $t$ ), covariance estimates for the location errors ( $\Delta x$ ,  $\Delta y$ ,  $\Delta z$ ), and the number of stations ( $N$ ) used are given for each final solution in Table 1. Additionally, the differences in geometric distance ( $\Delta R$ ) and time of occurrence ( $\Delta t$ ) between the X-ray and  $dE/dt$  sources are calculated for each pair. As seen in Table 1, each pair of X-ray/ $dE/dt$  sources is co-located in space by less than 50 m. As expected, the sequences of 3 natural sources and 4 triggered sources move downward with increasing time. Further, all differences in time of occur-

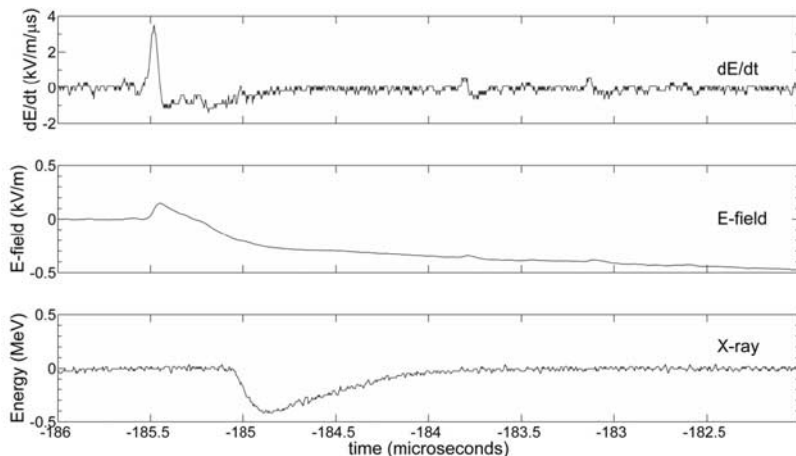


**Figure 4.** Station 1 waveforms (using atmospheric electricity sign convention) for one event during MSE-0604 at a distance of  $\sim 250$  m which illustrate the typical delay observed between (top)  $dE/dt$  and (bottom) X-ray detection. Comparison of the (middle) E-field, obtained by integrating  $dE/dt$ , and the X-ray waveform indicates that the X-ray emission is most likely associated with the electrostatic field change due to the leader step. The electrostatic field at ground becomes more negative as the stepped leader lowers negative charge towards ground, whereas the radiation field pulse at the start of the step, due to a current pulse, is of opposite sign to the electrostatic field change.

**Table 1.** Summary of the Location Results for Individual dE/dt and X-Ray Events<sup>a</sup>

Event	<i>x</i> (m)	<i>y</i> (m)	<i>z</i> (m)	<i>t</i> (μs)	$\Delta x$ (m)	$\Delta y$ (m)	$\Delta z$ (m)	<i>N</i>	$\Delta R$ (m)	$\Delta t$ (μs)
<i>MSE-0604 2 June 2006</i>										
dE/dt 1	241.2	-40.9	186.9	-188.830	3.2	4.4	4.0	5	48.7	0.322
X-ray 1	269.1	-60.9	152.4	-188.507	12.6	22.3	35.6	5	48.7	0.322
dE/dt 2	238.4	-62.6	108.4	-70.012	1.7	3.1	6.0	7	46.8	1.303
X-ray 2	282.2	-49.9	97.8	-68.708	26.2	88.2	143.3	5	46.8	1.303
dE/dt 3	250.6	-83.4	75.1	-17.032	1.1	1.8	4.3	7	49.5	0.217
X-ray 3	288.4	-110.0	57.5	-16.815	9.9	8.6	22.4	5	49.5	0.217
<i>UF-0707 31 July 2007</i>										
dE/dt 1	386.7	-236.9	140.5	-64.934	10.8	10.6	45.4	5	34.2	0.363
X-ray 1	353.3	-239.9	147.2	-64.571	30.6	29.0	164.9	5	34.2	0.363
dE/dt 2	381.8	-204.0	129.1	-17.366	3.4	3.1	16.7	5	32.9	0.113
X-ray 2	371.7	-191.1	100.6	-17.254	48.7	28.1	163.9	5	32.9	0.113
dE/dt 3	392.7	-195.0	89.7	-7.730	5.6	5.0	34.2	5	31.5	0.537
X-ray 3	380.3	-177.2	67.0	-7.193	8.3	8.6	32.1	5	31.5	0.537
dE/dt 4	389.6	-198.0	69.4	-4.141	2.9	2.7	22.4	5	39.0	0.624
X-ray 4	385.1	-169.1	43.6	-3.517	6.1	6.9	30.3	5	39.0	0.624

<sup>a</sup>The final two columns compare the location and time of occurrence for source pairs.

rence ( $\Delta t$ ) are of the same sign, meaning that each located X-ray source occurred after the corresponding dE/dt source. Figure 4 illustrates the delay typically observed in the X-ray emission by showing dE/dt and integrated dE/dt (electric field) waveforms on the same timebase with a corresponding X-ray burst at the same station. The delay observed in Figure 4 is not exactly the delay determined from the source solutions ( $\Delta t$ ), as the timing has not been adjusted for any possible differences arising from the propagation paths; nevertheless, including these adjustments would not alter the fact that the located X rays are emitted after the dE/dt peaks. For observations made very close to the leader tip (the measurements in Figure 4 are  $\sim 250$  m from the source), the positive dE/dt peak (radiation field) becomes small compared with the negative electrostatic field change that apparently drives the runaway electrons that produce the X rays.

#### 4. Conclusions

[10] The results presented here not only confirm previous reports on the association of X-ray emissions with negative downward leaders [Moore et al., 2001; Dwyer et al., 2003, 2004, 2005] but also quantify a close spatial and temporal relationship between the sources of X rays and leader step electric field changes. Further, Table 1 shows this relationship to be very similar for a first stroke natural lightning and a rocket-triggered lightning stroke. The delay observed in the locatable X rays and the peaks in the leader step field change indicates that the negative electrostatic field change is responsible for the X-ray emissions. Considering the physical mechanism for an individual downward leader step, in which there is probably a current pulse whose rate of change produces the radiation field, followed by the lowering of significant charge causing the electrostatic field, one might predict that the source of the X rays, runaway electrons, should be beneath the source of the electric field change. The results presented here cannot unequivocally confirm this hypothesis, but this view is not contradicted by the data presented. All but one of the seven source pairs in Table 1 have the X-ray source lower in the *z* coordinate than

the dE/dt source, and that lone pair has the two located 7 m apart; however, the uncertainties in the X-ray locations are relatively large. It is noteworthy that every difference in geometric distance ( $\Delta R$ ) for the source pairs of MSE-0604 contains a large *x* component in the same direction which comprises a significant portion of  $\Delta R$ . If this represents some systematic error in locating one of the source types, we can find no explanation for it.

[11] It should be noted that some X-ray emission may occur prior to the source responsible for the peak dE/dt. As seen in Figure 2, X rays (denoted by small arrows) are clearly detected at Station 3 and Station 5 prior to the arrival time used in the least squares algorithm. This phenomenon, which was observed for other events, usually occurs at the stations closest to the source. This observation may indicate an X-ray source with a time varying intensity, meaning that the X-ray emission is initially weak and becomes more intense after the leader process that causes the peak values in the associated dE/dt waveforms. It may be possible to obtain a clearer view of this early X-ray phenomenon, as well as improve the overall location accuracy for X-ray sources, by increasing the detector density and/or using scintillators with faster time response.

[12] **Acknowledgments.** This work was supported in part by DOT (FAA) grant 99-G-043 and NSF grants ATM 0003994, ATM 0346164, ATM 0420820, ATM 0133773, and ATM 0607885. We wish to thank Rob Olsen III for devising and helping implement the technique for measuring system time delays. We also thank David Thomas, a Florida registered land surveyor and mapper, for obtaining the local station coordinates.

#### References

- Dwyer, J. R., et al. (2003), Energetic radiation produced during rocket-triggered lightning, *Science*, 299, 694–697.
- Dwyer, J. R., et al. (2004), Measurements of x-ray emission from rocket-triggered lightning, *Geophys. Res. Lett.*, 31, L05118, doi:10.1029/2003GL018770.
- Dwyer, J. R., et al. (2005), X-ray bursts associated with leader steps in cloud-to-ground lightning, *Geophys. Res. Lett.*, 32, L01803, doi:10.1029/2004GL021782.
- Koshak, W. J., and R. J. Solakiewicz (1996), On the retrieval of lightning radio sources from time-of-arrival data, *J. Geophys. Res.*, 101, 26,631–26,639.
- Koshak, W. J., et al. (2004), North Alabama Lightning Mapping Array (LMA): VHF source retrieval algorithm and error analyses, *J. Atmos. Oceanic Technol.*, 21, 543–558.

Moore, C. B., K. B. Eack, G. D. Aulich, and W. Rison (2001), Energetic radiation associated with lightning stepped-leaders, *Geophys. Res. Lett.*, 28, 2141–2144.

Proctor, D. E. (1971), A hyperbolic system for obtaining VHF radio pictures of lightning, *J. Geophys. Res.*, 76, 1478–1489.

Thomas, R. J., P. R. Krehbiel, W. Rison, S. J. Hunyady, W. P. Winn, T. Hamlin, and J. Harlin (2004), Accuracy of the Lightning Mapping Array, *J. Geophys. Res.*, 109, D14207, doi:10.1029/2004JD004549.

Thomson, E. M., P. J. Medelius, and S. Davis (1994), A system for locating the sources of wideband  $dE/dt$  from lightning, *J. Geophys. Res.*, 22, 793–22,802.

Wilson, C. T. R. (1925), The acceleration of beta-particles in strong electric fields such as those of thunderclouds, *Proc. Cambridge Philos. Soc.*, 22, 534–538.

---

C. Biagi, D. Hill, J. Howard, and M. A. Uman, Department of Electrical and Computer Engineering, University of Florida, Gainesville, FL 32611, USA. (ironjoe@ufl.edu)

J. R. Dwyer, H. K. Rassoul, and Z. Saleh, Department of Physics and Space Sciences, Florida Institute of Technology, Melbourne, FL 32901, USA.

J. Jerauld, Raytheon Missile Systems, 1151 E Hermans Rd, Tucson, AZ 85706, USA.